NANO LETTERS

2008
Vol. 8, No. 3
931-934

Hierarchical Magnetite/Silica Nanoassemblies as Magnetically Recoverable Catalyst–Supports

Jianping Ge, Tuan Huynh, Yongxing Hu, and Yadong Yin*

Department of Chemistry, University of California, Riverside, California 92521

Received January 3, 2008; Revised Manuscript Received January 15, 2008

ABSTRACT

We report the synthesis of magnetically responsive hierarchical assemblies of silica colloids that can be used as recoverable supports for nanocatalysts. Each assembly is composed of a central magnetite/silica composite core and many small satellite silica spheres. The two regions are held together as a stable unit by a polymer network of poly(*N*-isopropylacrylamide). The central magnetite particles are superparamagnetic at room temperature with strong magnetic response to external fields, thus providing a convenient means for separating the entire assembly from the solution. The satellite silica particles provide large surface areas for loading nanocatalysts through the well-developed silane chemistry. As an example, we demonstrate the use of such magnetically responsive hierarchical assemblies as recoverable supports for Au nanocatalysts for the reduction of 4-nitrophenol with $NaBH_4$.

When used in liquid phase reactions, inorganic nanocatalysts immobilized on solid supports can combine high surface area with the additional benefit of relatively facile recovery and regeneration.[1,2] Ideally, the support material should also possess a high surface area to maximize catalyst loading and activity. Besides making the support porous,[3,4] it is also possible to increase specific surface area by shrinking the dimension of the support. Conventional separation methods, however, may become inefficient for support particle sizes below 100 nm. The incorporation of magnetic materials such as iron oxide into supports offers a solution to this problem.[5–9] Unfortunately, the requirements for high surface area and fast separation seem to be also contradictory to each other for the magnetic particle based supports. On one hand, small superparamagnetic nanoparticles such as iron oxide has satisfactory specific surface area, but the weak magnetic response makes it difficult to efficiently separate them from solution using moderate magnetic field gradients.[10,11] On the other hand, embedding many of them in microspheres may improve separation, but it will also significantly decrease the surface area for catalyst loading. One practical strategy to tackle this problem is to form composite nanostructures with two kinds of functional substructures, which respectively favor the high surface area and convenient magnetic separation.

In this paper, we report the synthesis of hierarchical assemblies of silica colloids, which possess both high separation efficiency and relatively high surface area, making them ideal recoverable supports for nanocatalysts. As shown in Figure 1, the center of each assembly is a silica coated magnetite (Fe_3O_4) core, which is composed of many 10 nm crystallites and thus displaying superparamagnetism at room temperature.[12,13] The Fe_3O_4 cores strongly interact with external magnetic fields and can be easily separated from solution in a low magnetic field gradient (<30 T/m). After the cores are grafted with a thick layer of poly(*N*-isopropylacrylamide) (p-NIPAM), many satellite silica spheres are then synthesized, which form stable assemblies around each magnetic core as sterically confined by the polymer network. The large surface area associated with the small size (<70 nm) of satellite silica particles ensures a high loading of nanocatalysts. The well-developed silane chemistry also

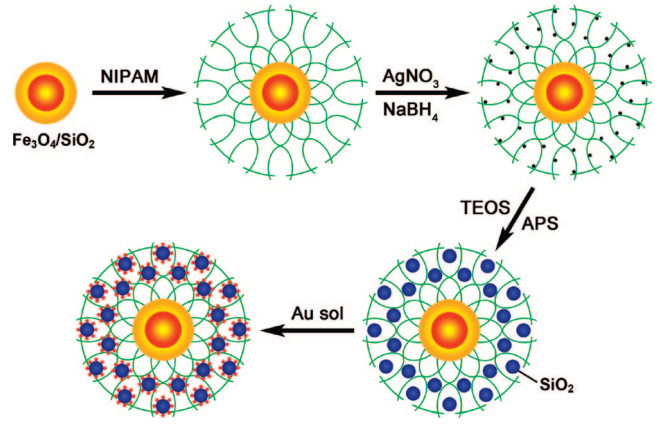

Figure 1. Schematic illustration of the synthetic procedure from Fe_3O_4/SiO_2 colloids to Fe_3O_4/SiO_2/p-NIPAM/SiO_2-Au assemblies.

* To whom correspondence should be addressed. E-mail: yadong.yin@ucr.edu

10.1021/nl080020f CCC: $40.75
Published on Web 02/01/2008

allows the silica surface to be functionalized to immobilize a large number of nanocatalysts of various compositions.[14–18] It is certainly possible to directly use silica coated Fe_3O_4 colloids to load catalyst particles, however, the requirement of efficient separation makes it difficult to shrink the overall size (~200 nm) of the support particles to meet the other requirement of large surface areas. The strategy of forming composite structures containing both magnetic component for efficient separation and small silica colloids for high catalyst loading may provide a practical route to reconcile the seemingly contradictory requirements. An additional advantage of such system is that the satellite silica can be potentially changed to other support materials such as titania and zirconia after some minor modifications to the synthetic procedure, thus utilizing the support−catalyst interaction for further improving the reactivity and selectivity.[19–25] Here, we choose gold nanocrystals as the catalytic component to demonstrate the use of magnetically responsive hierarchical assemblies as nanocatalyst–supports.

Figure 1 outlines the procedure we used to synthesize the Fe_3O_4/SiO_2/p-NIPAM/SiO_2-Au assemblies. Superparamagnetic Fe_3O_4 colloids (~100 nm) were synthesized using a high temperature hydrolysis process.[12] After being coated by a layer of silica through a sol–gel process (Figure S1a, Supporting Information), particle surfaces were further functionalized with a monolayer of [3-(methacryloyloxy)propyl]trimethoxysilane (MPS) through the siloxane linkage.[26] An aqueous phase precipitation polymerization process was used to form a robust polymer coating on the core surfaces by copolymerizing surface MPS with NIPAM (monomer) and *N*,*N*′-methylenebisacrylamide (MBA, cross-linker).[27] As the reaction temperature (70 °C) is above the lower critical solution temperature (LCST, typically 32 °C) of p-NIPAM, the growing polymer chains collapse onto the silica surface to form a polymeric shell. At room temperature, the polymer chains become hydrophilic and the composite colloids disperse well in water and alcohols. Both optical microscopy observations and dynamic light scattering (DLS) measurements suggest the formation of separate composite colloids with a relatively thick coating of polymer on each Fe_3O_4/SiO_2 core (Figure S2, Supporting Information). The p-NIPAM shell also shows a characteristic thermosensitive size change at around 33 °C. The polymer shell is not easily distinguishable in TEM due to its low contrast, but its presence can be still evidenced by significantly increased interparticle separations (in comparison to the original Fe_3O_4/SiO_2 particles) when the colloids are deposited on solid substrates such as TEM grids (Figure S1b, Supporting Information).

After swelling Fe_3O_4/SiO_2/p-NIPAM colloids in an aqueous solution of $AgNO_3$, Ag nanoparticles were directly synthesized inside the polymer network through in situ reduction with $NaBH_4$ (Figure 2a,b). This "Ag^+ absorption–reduction" process can be repeated to increase number density of Ag particles embedded in the polymer shells. An additional sol–gel process was performed to form satellite silica by using Ag nanoparticles as templates, producing Fe_3O_4/SiO_2/p-NIPAM/SiO_2 assemblies (Figure 2c,d). A very small amount of SiO_2 particles produced outside the polymer via homogeneous nucleation has also been observed, and they can be conveniently removed by magnetic separation process. Careful inspection of the satellite silica may reveal voids at the center of some of these particles, which were due to the dissolution of silver nanoparticles in excess ammonia over a long period of reaction. It is clear that the silica satellites are trapped inside the polymer network around each central Fe_3O_4/SiO_2 particle but not simple aggregations through surface siloxane linkages. By controlling the cross-linking density of the polymer network according to the size of the silica satellites, it is possible to fully retain the silica particles in the polymer shell and prevent significant loss of active materials during the catalytic reactions. We have also been able to vary the size and number density of silica satellites by controlling the loading of Ag nanoparticles: if Ag particle loading is increased with other parameters being fixed, the diameter of satellite silica particles decreases and their number density increases (Figure S3, Supporting Information). Such structural manipulation allows for optimization of catalytic activity.

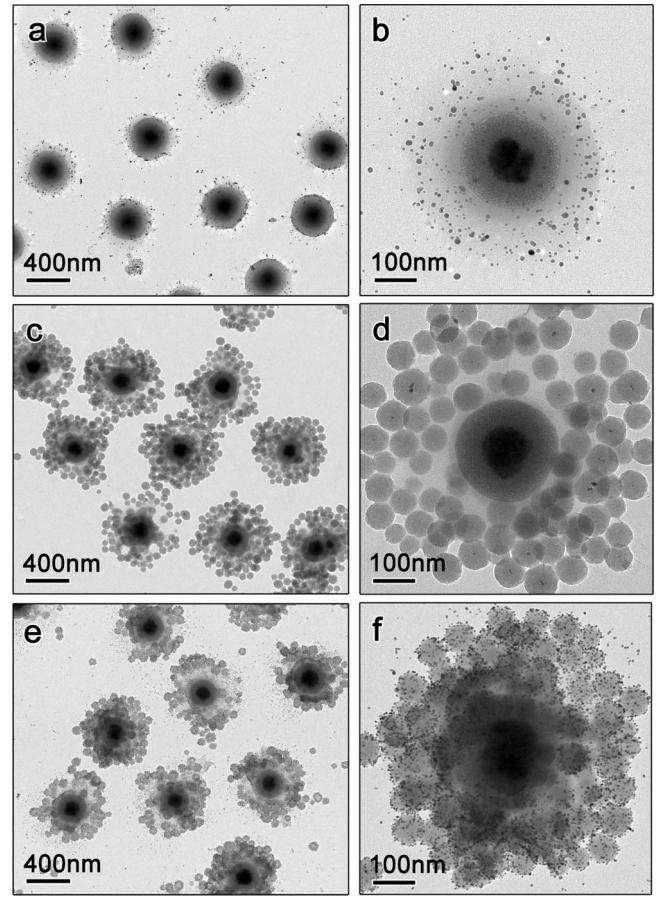

Figure 2. TEM images showing the evolution of hierarchical assemblies in the later three steps: (a,b) Fe_3O_4/SiO_2/p-NIPAM/Ag, (c,d) Fe_3O_4/SiO_2/p-NIPAM/SiO_2, and (e,f) Fe_3O_4/SiO_2/p-NIPAM/SiO_2-Au.

We chose Au-catalyzed reduction of 4-nitrophenol (4-NP) in the presence of $NaBH_4$ as a model system to demonstrate the use of our complex assemblies as recoverable catalyst–supports.[28,29] The substrates and products of this reaction are

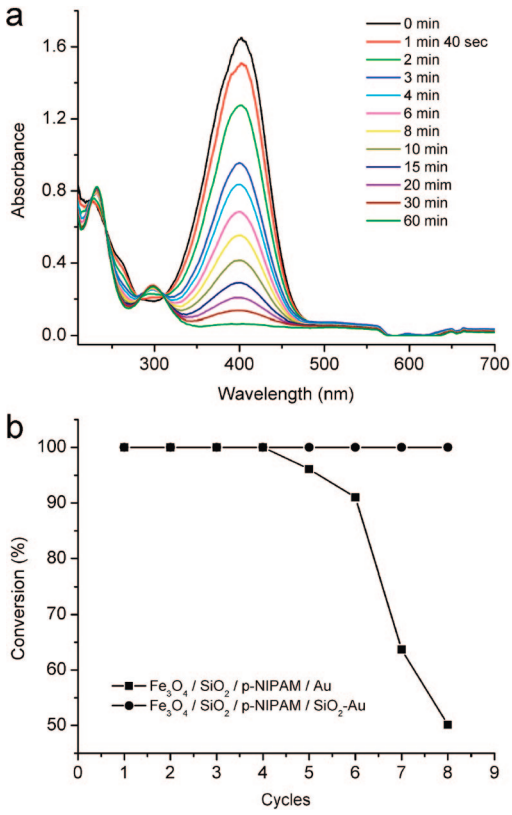

Figure 3. (a) UV–vis spectra showing the gradual reduction of 4-NP with Fe_3O_4/SiO_2/p-NIPAM/SiO_2-Au catalyst. (b) Conversion of 4-NP in eight successive cycles of reduction and magnetic separation with two types of catalysts.

easily detected by spectroscopic methods, and there is no appreciable byproduct formation. Au nanocatalysts with an average diameter of 5 nm were prepared by reducing $HAuCl_4$ with $NaBH_4$ in an aqueous solution in an ice bath. Because no strong capping agent was involved in the original synthesis, the Au particles can be easily immobilized on the silica satellites through the gold−amine complexation by using 3-aminopropyl-triethoxysilane (APS) as the coupling agent (Figure 2e,f).[30] It is worth noting that the catalyst loading could be simply tuned by controlling the amount of Au nanoparticles introduced into the system (Figure S4, Supporting Information).

Without Au catalyst, the reduction reaction does not proceed even in a large excess of $NaBH_4$, as evidenced by a nonvarying absorption spectrum with the major peak located at 400 nm, a wavelength characteristic of 4-nitrophenolate ions. However, when a trace amount of as-made catalyst was introduced into the solution, the absorption at 400 nm decreases and absorption at 295 nm increases gradually, indicating the reduction of 4-NP and formation of 4-aminophenol (4-AP), respectively. Because the concentration of catalyst is very low, light scattering caused by carrier colloids does not interfere with the absorption measurements. Figure 3a shows the UV−vis spectra as a function of reaction time for a typical reduction process. Visually, the bright-yellow solution gradually becomes colorless over 60 min, indicating complete conversion of 4-NP.

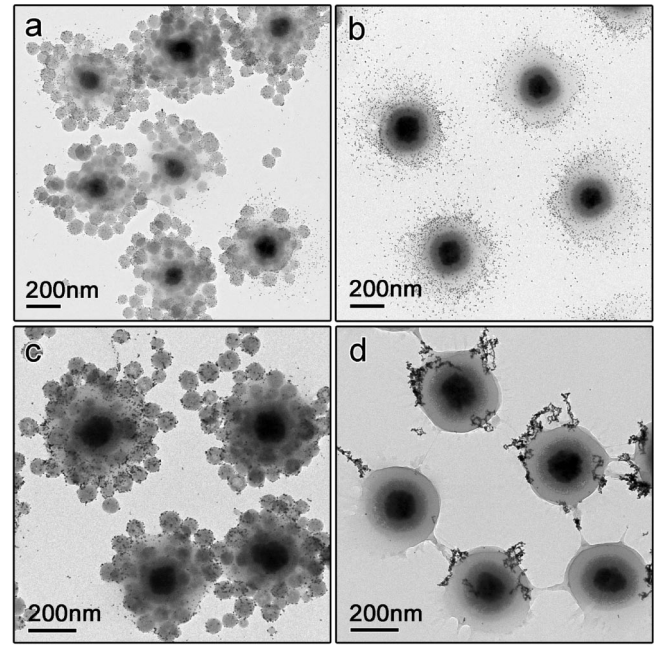

Figure 4. TEM images showing the morphology changes of (a,c) Fe_3O_4/SiO_2/p-NIPAM/SiO_2-Au and (b,d) Fe_3O_4/SiO_2/p-NIPAM/Au catalysts before (a,b) and after (c,d) the first cycle of catalysis.

To demonstrate magnetic recovery of the assemblies, we increased the concentration of reagents and catalysts by 50 times so that the reaction can complete within ~10 min. In each cycle, after 5 min of reaction, the sample was diluted 50 times for UV−vis measurements in order to determine the conversion of 4-NP. Then catalysts were quickly separated from solution using a NdFeB magnet (Figure S5b, Supporting Information), rinsed with deionized (DI) water, and dispersed into DI water for the next cycle of catalysis. As shown in Figure 3b, the catalyst can be successfully recycled and reused in eight successive reactions, all with conversions of 100% within 5 min periods. The conversion starts to decrease after ~10 cycles, probably due to gradual loss of catalytic assemblies with repeated magnetic separation.

The satellite silica spheres significantly enhance the stability of Au nanocatalysts under reaction conditions.[15] For comparison, Au nanoparticles were also directly incorporated into polymer shells of Fe_3O_4/SiO_2/p-NIPAM colloids with the same catalyst loading as for Fe_3O_4/SiO_2/p-NIPAM/SiO_2 assemblies (Figure 4b). The conversion rate using such catalysts decreases dramatically after each additional cycle of reactions. As shown in Figure 3b, the total conversion within the first 5 min drops rapidly after only four reaction cycles. The aggregation of Au particles inside the polymer network seems to be the major cause for the sharp decrease of catalytic activity. Au particles on Fe_3O_4/SiO_2/p-NIPAM colloids were found to be severely aggregated after the first reaction cycle (Figure 4b,d), while those supported on Fe_3O_4/SiO_2/p-NIPAM/SiO_2 colloids did not show obvious changes (Figure 4a,c). Apparently, the strong complexation between Au and amine groups stabilizes the catalysts on the silica surfaces and prevents their detachment and subsequent aggregation.

In summary, we have demonstrated the fabrication of hierarchical assemblies of silica colloids and their use as recoverable supports for nanocatalysts. The composite structures possess relatively high surface area and can be conveniently separated from reaction solution and recovered using external magnetic fields. The magnetic nanocomposite catalyst system demonstrated here is expected to find many industrially important catalytic applications.[19,31–33] Further fine-tuning of the structure of such system may provide other opportunities in optimizing the performances of the catalysts. For example, the polymer networks can be further engineered and potentially used as selective gates to control access of reactants to the nanocatalysts.[28,34,35]

Acknowledgment. Y. Yin thanks the University of California, Riverside for start-up funds and the Regents' Faculty Fellowship. We also thank Dr. Benjamin Gilbert for help with dynamic light scatting measurements and Dr. C. K. Erdonmez for comments on the manuscript.

Supporting Information Available: Experimental procedures, Photos of separation process, TEM images of Fe_3O_4/SiO_2 and Fe_3O_4/SiO_2/p-NIPAM particles, Fe_3O_4/SiO_2/p-NIPAM/Au catalyst, and silica satellites and Au at controllable loadings. This material is available free of charge via the Internet at http://pubs.acs.org.

References

(1) Ko, S.; Jang, J. *Angew. Chem., Int. Ed.* **2006**, *45*, 7564–7567.
(2) Yoon, B.; Wai, C. M. *J. Am. Chem. Soc.* **2005**, *127*, 17174–17175.
(3) Jiang, Y.; Gao, Q. *J. Am. Chem. Soc.* **2006**, *128*, 716–717.
(4) Teng, X. W.; Liang, X. Y.; Rahman, S.; Yang, H. *Adv. Mater.* **2005**, *17*, 2237–2241.
(5) Stevens, P. D.; Li, G.; Fan, J.; Yen, M.; Gao, Y. *Chem. Commun.* **2005**, 4435–4437.
(6) Wang, L.; Yang, Z.; Gao, J.; Xu, K.; Gu, H.; Zhang, B.; Zhang, X.; Xu, B. *J. Am. Chem. Soc.* **2006**, *128*, 13358–13359.
(7) Yi, D. K.; Lee, S. S.; Ying, J. Y. *Chem. Mater.* **2006**, *18*, 2459–2461.
(8) Jeong, U.; Teng, X.; Wang, Y.; Yang, H.; Xia, Y. *Adv. Mater.* **2007**, *19*, 33–60.
(9) Xu, R.; Xie, T.; Zhao, Y.; Li, Y. *Nanotechnology* **2007**, *18*, 055602.
(10) Fletcher, D. *IEEE Trans. Magn.* **1991**, *27*, 3655–3677.
(11) Yavuz, C. T.; Mayo, J. T.; Yu, W. W.; Prakash, A.; Falkner, J. C.; Yean, S.; Cong, L.; Shipley, H. J.; Kan, A.; Tomson, M.; Natelson, D.; Colvin, V. L. *Science* **2006**, *314*, 964–967.
(12) Ge, J.; Hu, Y.; Biasini, M.; Beyermann, W. P.; Yin, Y. *Angew. Chem., Int. Ed.* **2007**, *46*, 4342–4345.
(13) Ge, J.; Hu, Y.; Yin, Y. *Angew. Chem., Int. Ed.* **2007**, *46*, 7428–7431.
(14) Graf, C.; Dembski, S.; Hofmann, A.; Ruhl, E. *Langmuir* **2006**, *22*, 5604–5610.
(15) Ketelson, H. A.; Brook, M. A.; Pelton, R.; Heng, Y. M. *Chem. Mater.* **1996**, *8*, 2195–2199.
(16) Kim, J.; Lee, J. E.; Lee, J.; Jang, Y.; Kim, S.-W.; An, K.; Yu, J. H.; Hyeon, T. *Angew. Chem., Int. Ed.* **2006**, *45*, 4789–4793.
(17) Liu, N.; Prall, B. S.; Klimov, V. I. *J. Am. Chem. Soc.* **2006**, *128*, 15362–15363.
(18) Pastoriza-Santos, I.; Gomez, D.; Pérez-Juste, J.; Liz-Marzán, L. M.; Mulvaney, P. *Phys. Chem. Chem. Phys.* **2004**, *6*, 5056–5060.
(19) Hashmi, A. S. K.; Hutchings, G. J. *Angew. Chem., Int. Ed.* **2006**, *45*, 7896–7936.
(20) Davis, R. J. *Science* **2003**, *301*, 926–927.
(21) Prati, L.; Rossi, M. *J. Catal.* **1998**, *176*, 552–560.
(22) Biella, S.; Prati, L.; Rossi, M. *J. Catal.* **2002**, *206*, 242–247.
(23) Porta, F.; Prati, L.; Rossi, M.; Coluccia, S.; Martra, G. *Catal. Today* **2000**, *61*, 165–175.
(24) Qi, C.; Akita, T.; Okumura, M.; Haruta, M. *Appl. Catal., A* **2001**, *218*, 81–89.
(25) Biswait, C.; Bravo-Suárez, J. J.; Daté, M.; Tsubota, S.; Haruta, M. *Angew. Chem., Int. Ed.* **2006**, *45*, 412–415.
(26) Ge, J.; Hu, Y.; Zhang, T.; Yin, Y. *J. Am. Chem. Soc.* **2007**, *129*, 8974–8975.
(27) Gao, H.; Yang, W.; Min, K.; Zha, L.; Wang, C.; Fu, S. *Polymer* **2005**, *46*, 1087–1093.
(28) Lu, Y.; Mei, Y.; Drechsler, M.; Ballauff, M. *Angew. Chem., Int. Ed.* **2006**, *45*, 813–816.
(29) Panigrahi, S.; Basu, S.; Praharaj, S.; Pande, S.; Jana, S.; Pal, A.; Ghosh, S. K.; Pal, T. *J. Phys. Chem. C* **2007**, *111*, 4596–4605.
(30) Liz-Marzan, L. M.; Giersig, M.; Mulvaney, P. *Langmuir* **1996**, *12*, 4329–4335.
(31) Crooks, R. M.; Zhao, M.; Sun, L.; Chechik, V.; Yeung, L. K. *Acc. Chem. Res.* **2001**, *34*, 181–190.
(32) Narayanan, R.; El-Sayed, M. A. *J. Am. Chem. Soc.* **2003**, *125*, 8340–8347.
(33) Shokouhimehr, M.; Piao, Y.; Kim, J.; Jang, Y.; Hyeon, T. *Angew. Chem., Int. Ed.* **2007**, *46*, 7039–7043.
(34) Niu, Y.; Yeung, L. K.; Crooks, R. M. *J. Am. Chem. Soc.* **2001**, *123*, 6840–6846.
(35) Oh, S. K.; Niu, Y.; Crooks, R. M. *Langmuir* **2005**, *21*, 10209–10213.

NL080020F